parisons could be accomplished, and is offered with these limitations only because of the balancing urgency on the reporting of principal results.

The dynamic range of the dual-frequency experiment in terms of electron concentration at Venus is seen from Fig. 3 to be more than three orders of magnitude. The precision is variable, depending on whether dispersive Doppler or amplitude measurements are used in the analysis. Caustics cause particularly difficult problems and were certainly encountered on the day side and probably on the night side near the main ionization peak. In a future flight it would be valuable to have a second dispersive Doppler comparison (between 423.3 Mhz and S-band, for example) so that all of the levels of ionization could be measured with the high precision of this type of measurement.

Perhaps the most important single result of the dual-frequency experiment was the discovery of the dayside plasmapause inside which interplanetary magnetic field lines are expected to be entrapped. The Venus magnetic trap, and the light and radiowave trap in the superrefractive atmosphere, are features of special interest for further study and analysis. It seems very likely that Mars also has an induced magnetosphere, magnetopause, and plasmapause due to the solar wind. Mars appears to be without appreciable self-magnetism, and it has a conducting daytime ionosphere comparable to that of Venus (*12*). The sensitivity of a dispersive Doppler experiment may be required for its detection (*1*). There appear to be three different types of interaction of planetary bodies with the magnetoplasma of the solar wind, with Earth representing one, Moon a second, and Venus and Mars a third class. These differ because of planetary magnetism (Earth), high ionospheric conductivity and an atmosphere but no magnetism (Venus and Mars), and no magnetism, no atmosphere, and low conductivity (Moon).

MARINER STANFORD GROUP
Center for Radar Astronomy, Stanford University, Stanford, California, and *Stanford Research Institute, Menlo Park, California*

References and Notes

1. G. Fjeldbo, V. R. Eshleman, O. K. Garriott, F. L. Smith III, *J. Geophys. Res.* **70**, 3701 (1965); G. Fjeldbo and V. R. Eshleman, *Final Rep.*, contract NGR-05-020-065, *SU-SEL-67-109*, Stanford Electronics Laboratories, Stanford, California, November 1967.
2. A. J. Kliore *et al.*, *Science*, this issue.
3. C. W. Snyder, *ibid.*, this issue.
4. M. Ash, I. I. Shapiro, W. B. Smith, *Astron. J.* **72**, 338 (1967).
5. C. Barth *et al.*, *Science*, this issue.
5a. H. S. Bridge *et al.*, *ibid.*, this issue.
6. T. Gold, in *The Solar Wind*, R. L. Mackin and M. Neugebauer, Eds. (Pergamon, Oxford, 1966), pp. 381–389.
7. D. S. Colburn, R. G. Currie, J. D. Kihalov, C. P. Sonett, *Science* **158**, 1040 (1967); N. F. Ness, K. W. Behannon, C. S. Scearce, S. C. Cantarano, *J. Geophys. Res.* **72**, 5769 (1967); F. S. Johnson, J. E. Midgeley, *ibid.*, in press.
8. A. J. Dessler, in *Atmospheres of Venus and Mars*, J. C. Brandt and M. B. McElroy, Eds. (Gordon and Breach, London, 1967), pp. 241–250.
9. W. I. Axford, *Planetary Space Sci.* **12**, 719 (1964).
10. F. S. Johnson, private communication.
11. *Pravda*, No. 295 (17977), 22 October 1967; G. Fjeldbo, paper presented before the 5th Aerospace Sciences Meeting, New York, January 1967; V. R. Eshleman, *Science* **158**, 585 (1967).
12. E. J. Smith, L. Davis, Jr., P. J. Coleman, Jr., D. E. Jones, *Science* **149**, 1241 (1965); A. J. Kliore, D. L. Cain, G. S. Levy, V. R. Eshleman, G. Fjeldbo, F. D. Drake, *ibid.*, p. 1243.
13. We thank the NASA Headquarters Mariner Program Office under the direction of Glenn A. Reiff for continuous encouragement and support over the past 2 years, and the many technical and scientific personnel at Jet Propulsion Laboratory who, under the direction of Dan Schneiderman, Project Manager, and Conway Snyder, Project Scientist, made the successful integration of Stanford's receiver possible. Research support was funded under JPL 951520.
14. Principal and co-investigators for the dual-frequency radio occultation experiment are: V. R. Eshleman, G. Fjeldbo, H. T. Howard, and B. B. Lusignan of Stanford University, R. L. Leadabrand and R. A. Long of the Stanford Research Institute, and A. M. Peterson of both organizations. Other key personnel are B. C. Fair and R. I. Presnell of SRI and W. E. Faulkerson and G. L. Tyler of SU. Many others contributed significantly, including R. Merritt, L. Raley, and A. Sader. The principal investigator acknowledges in particular the role of Howard as overall project manager and director of ground-based operations, of Long as the responsible engineer for the spacecraft receiver, and of Fjeldbo for data reduction and scientific planning and analysis.

11 December 1967

Atmosphere and Ionosphere of Venus from the Mariner V S-Band Radio Occultation Measurement

Abstract. *Measurements of the frequency, phase, and amplitude of the S-band radio signal of Mariner V as it passed behind Venus were used to obtain the effects of refraction in its atmosphere and ionosphere. Profiles of refractivity, temperature, pressure, and density in the neutral atmosphere, as well as electron density in the daytime ionosphere, are presented. A constant scale height was observed above the tropopause, and the temperature increased with an approximately linear lapse rate below the tropopause to the level at which signal was lost, presumably because heavy defocusing attenuation occurred as critical refraction was approached. An ionosphere having at least two maxima was observed at only 85 kilometers above the tropopause.*

On 19 October 1967, the Mariner V space probe passed within about 4100 km of the surface of Venus. Its trajectory had been designed so that the craft as observed from Earth appeared to pass almost diametrically behind the planet. About 3 minutes before the closest approach time, the S-band radio beam emanating from the paraboloidal high-gain antenna of the probe began to enter the sensible neutral atmosphere on the dark side of Venus with a relative velocity of about 7.3 km/sec, at a radial distance of about 6145 km from the center. At the point of tangency, the latitude was about 37°N, and the solar zenith angle was 142.3°. As the beam penetrated the atmosphere, refraction caused the path of propagation to deviate from a straight line, and the velocity of propagation to vary from the speed of light in free space. In addition, the lenslike effect of the gradient of refractivity caused defocusing, which spread the power in the beam over a greater angular width, and caused the signal power received at Earth to decrease. These effects were observed as changes in the frequency, phase, and signal strength received during this period at the tracking stations on Earth.

As the beam penetrated deeper into the dense atmosphere of Venus these effects became more pronounced, until at about 2 minutes and 40 seconds past the closest approach time the received signal strength gradually descended below the threshold of the receiver apparatus. This indicated that, rather than being physically interrupted by the limb of the planet, the signal was gradually extinguished by rapidly increasing refractive defocusing as the critical refraction level was approached.

Approximately 15 minutes later, the signal again began to be discernible as the radio beam emerged from behind the sunlit side of the planet and began to rise through the atmosphere. The latitude at this point was about 32.4°S, and the solar zenith angle was 33.3°. Effects similar to those that occurred during the entry into occultation were again observed, except that a very strong effect of an ionosphere was observed during the exit on the daytime side. About 23 minutes after closest approach, the radio beam left the atmosphere of Venus, and the frequency, phase, and amplitude characteristics of the signal returned to those observed in free space.

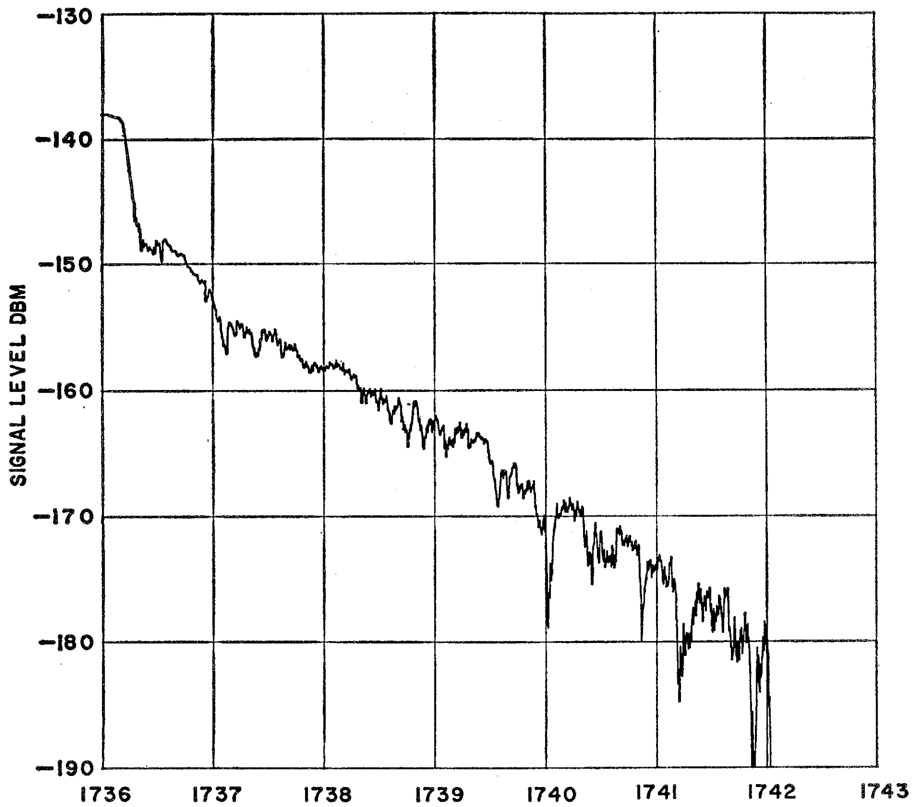

Fig. 1. Received signal strength as a function of time during entry into occultation.

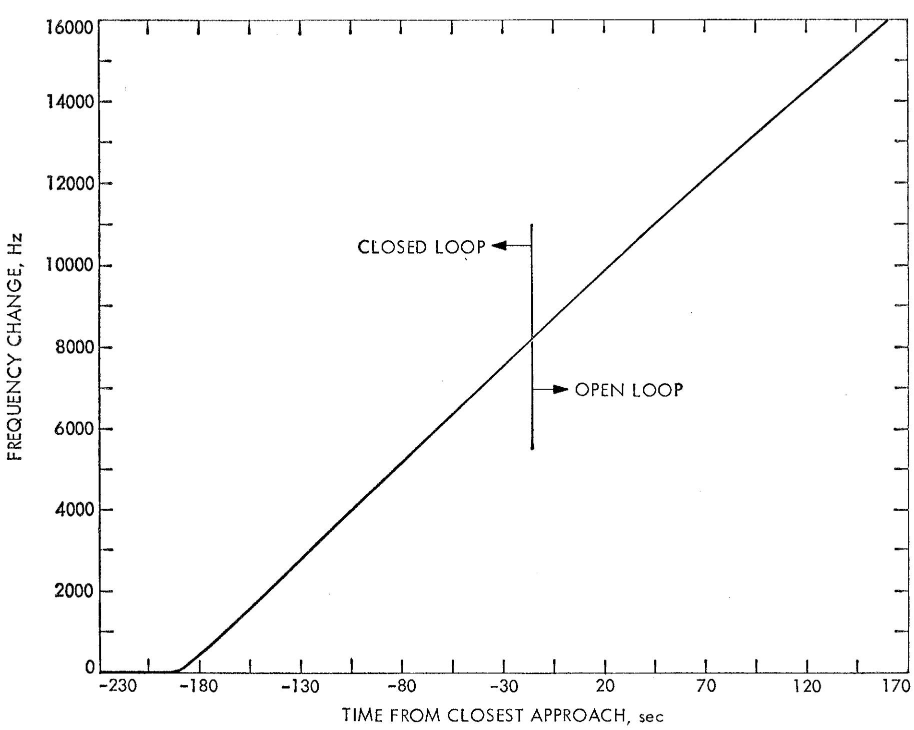

Fig. 2. Frequency residuals from data taken during entry into occultation. Time is referenced to the time of closest approach.

The experiment described above is similar to the one performed at Mars with Mariner IV in 1965 (*1*); however, certain significant differences were necessitated by the different nature of the Venus atmosphere as compared with that of Mars.

In the case of Mars, the experiment was performed in the so-called two-way mode, so that a frequency referenced by a rubidium standard (stable to about 1 part in 10^{12}) was transmitted to the probe, where it was coherently retransmitted by a transponder. Thus, the signal received on the ground had completed two traversals of the atmosphere of Mars, and the effects of these traversals could very precisely be measured by comparison to the very stable frequency reference. In preparing for the Venus experiment, however, it was felt that, because of the high frequency rates and massive defocusing attenuation, it would be unwise to risk the loss of lock in the spacecraft receiver during a critical data period. For this reason, it was decided to carry out all of the entry portion of the experiment and most of the exit portion in the one-way mode, in which the frequency transmitted by the probe is referenced to an on-board crystal oscillator, which is inherently less stable. However, as borne out in the data, the stability of the oscillator was sufficient for the Venus experiment. It was attempted to establish two-way lock after leaving the neutral atmosphere on exit in order to probe the ionosphere more precisely, but because of rapid changes in frequency rate and uncertainties in the predicted time of leaving the neutral atmosphere, two-way lock was not reestablished until some time later.

Another significant change involved the high-gain antenna of the probe (*2*). If it had pointed directly at Earth in free space, then it would have performed poorly during the occultation, because the refracted radio beam would have emanated from a position on the antenna differing from the boresight position by the amount of the refractive bending angle, and the gain of the antenna would have been reduced at a time when maximum gain was needed to overcome increasing refractive defocusing. To counteract this problem, a movable high-gain antenna was used. It initially was positioned to

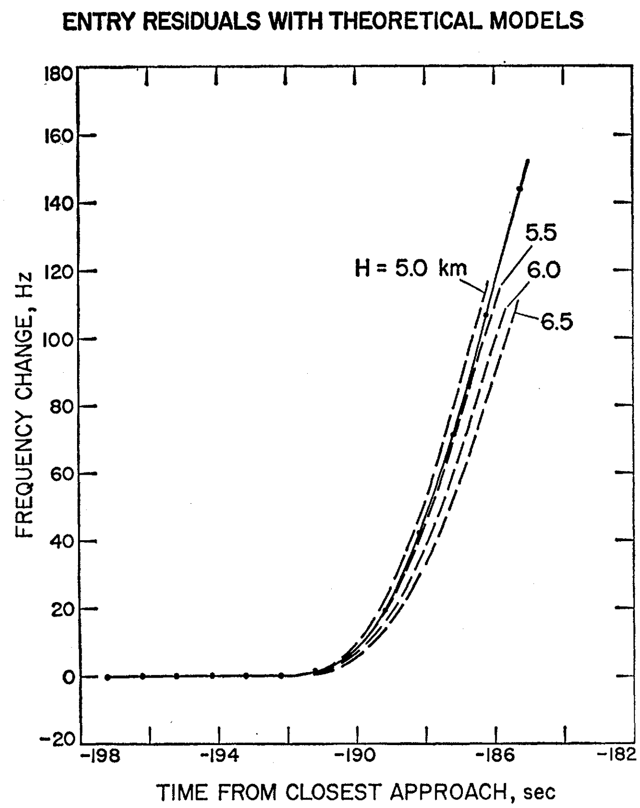

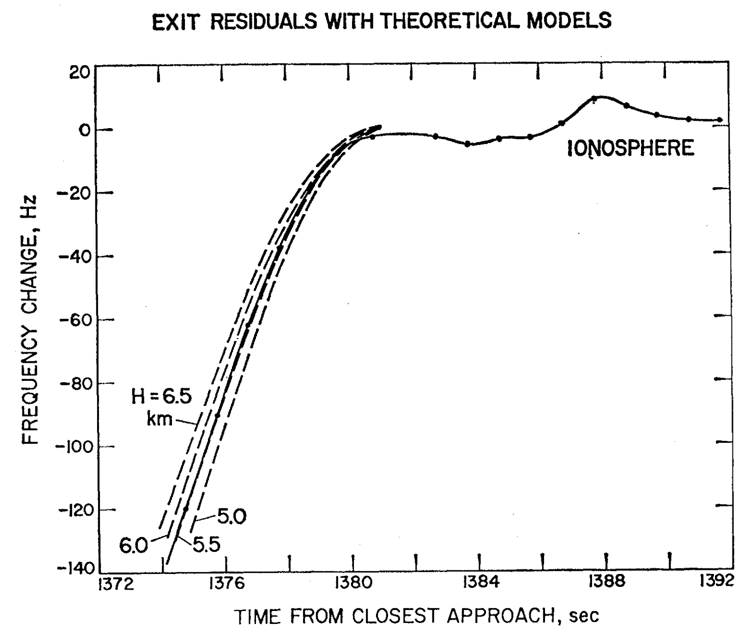

Fig. 3 (left). Frequency residuals at the inception of atmospheric effects at entry compared to theoretical predictions for the case of constant scale height. Fig. 4 (above). Frequency residuals at the termination of atmospheric effects at exit. The *s*-shaped feature is caused by the daytime ionosphere.

point about 8.2° away from Earth, in the direction of the expected bending. While the probe was behind the planet, a signal from a terminator sensor initiated a positioning change which moved the antenna axis to a position offset by 9.7° in the opposite direction in order to improve the gain during the exit portion of the data. In addition to increasing the amount of data collected by the S-band experiment, this pointing angle change also improved tracking coverage.

Data for the Mariner V experiment were received at all four of the NASA/JPL Deep Space Net Stations at Goldstone, California. The major differences between the ground station equipment used for the Mariner IV Occultation experiment (*1–3*) and that used for Mariner V were due to the availability of more sensitive receiving equipment and the differences in the expected rate of change of frequency.

The 210-foot (63 m) Advanced Antenna System (AAS) was used as the prime station for both open- and closed-loop data. The system temperature of this station was 28°K at the encounter elevation angle. The closed loop receiver was in the normal station configuration in which the Doppler extractor and resolver were used to obtain frequency in a digital form, and automatic gain control voltage was used to indicate received signal level, both in real time.

The closed-loop data were then processed through the Jet Propulsion Laboratory (JPL) Orbit Determination Program, which removed all effects except those caused by the atmosphere of Venus. Since these data were based on a nondestructive cycle count, the summing of the frequency residuals yielded a precise measurement of the total phase-path change in cycles. These data were then used to obtain the results described later in this report.

The open-loop data were obtained in the form of a wide-band predetection-analog magnetic-tape recording from a fixed-tuned receiver. This recording had a bandwidth in excess of 100 khz. This wide bandwidth was required because of the high rate of change of frequency due to the orbit and because of the effects due to the planetary atmosphere. The analog magnetic tape was digitized by slowing the original tape from 60 down to 3¾ inches per second so that the the 320-khz synchronizing tone was reduced to 20 khz, which was used to trigger the digitizer. The data were reduced first by narrow-band filtering of the signal, thereby permitting a great reduction in the amount of data to be processed. A digital spectral analysis program was used to determine the time-frequency function, which was then used to run a digital local oscillator to minimize the rate of change of frequency.

A digital phase-lock loop program was then used to obtain the remaining frequency changes. These were compared to predictions based on the orbit, and the residuals due only to the atmosphere were computed. The received signal level, as a function of time, was also obtained from the phase-lock loop program, and is shown in Fig. 1. The undulations that appear in the received signal apparently have their sources in the atmosphere of Venus, resulting from phenomena such as focusing and defocusing by changing gradients. The closed-loop receiver at the AAS site lost lock at about 17 : 39 : 07 U.T., but the open-loop data extends to about 17 : 42 : 05. The combined open-loop and closed-loop data obtained during entry are shown in Fig. 2. Similar data were obtained during exit, except that a smaller percentage was obtained by the closed-loop receivers.

In addition to the AAS two operational 85-foot (25.5 m) antenna stations at Goldstone provided backup capacity for closed-loop operation, and the Venus Site 85-foot antenna had a new low-noise system, with a system temperature of 16.5°K which provided an open-loop backup capability.

The data were analyzed by two basically different approaches, both having the same objective—to find the profile of index of refraction (or refractivity) as a function of height in the atmosphere from data which basically consist of measurements of frequency or phase residuals at certain specified times.

The most direct method makes use of the trajectory of the probe to establish the connection between time and geometry, and then uses direct inversion of the integral equation describing the ray-optical refraction effects to obtain directly the profile of refractivity in the atmosphere (*4, 5*). This method is completely general, since no a priori assumptions regarding the analytical form of the refractive index profile have to be made.

The other method, referred to as pseudoinversion, is based on a step-by-step "construction" of a profile of refractivity to match the observed phase-delay data. It makes use of certain properties of planetary atmospheres that can be expected to apply also in the atmosphere of Venus. In the upper levels of the atmosphere, the temperature is assumed to be constant above some predetermined altitude, and the refractivity function is therefore an exponential with constant scale height. Once the refractivity at this reference altitude (which can be chosen arbitrarily) is determined by adjusting until computed and observed data match, the refractivity in each succeeding interval of height of arbitrary thickness is represented by an expression valid for a linearly changing scale height, and the rate of change of scale height is adjusted until convergence is achieved.

Figures 3 and 4 show frequency residuals obtained at the very top of the atmosphere during entry and exit, respectively. Theoretical predictions based on constant scale-height (isothermal) models are superimposed as dashed curves on the observed data, represented by the dots. Figure 3 shows that the actual data are quite consistent with a constant scale height of about 5.4 km for the first 20 to 30 km of the sensible upper neutral atmosphere. The exit data appear to be similar; however, they include the effects of a rather intense daytime ionosphere, which must be removed before the neutral atmosphere itself can be investigated.

Because of uncertainties in trajectory a probable error of ±0.2 km can be assigned to the measurement of scale height in the upper atmosphere. This yields a range of ratio of temperature to mean molecular weight of about 5.49 to 5.9. On the basis of the solar constant at the orbit of Venus and of the observed albedo of the planet, the effective temperature is computed to be about 230°K. Since this temperature would correspond to some level above the visible tops of the clouds, it can be argued that, at the altitude at which occultation measurements begin (about 6150 km from the planet center), the actual temperature

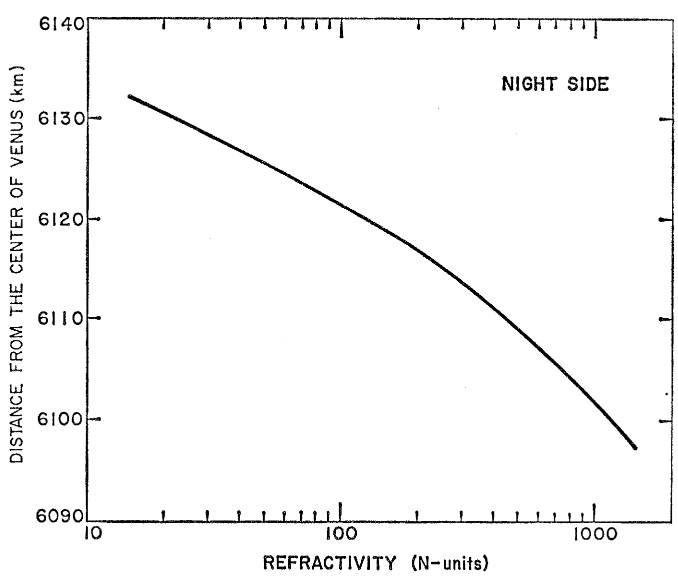

Fig. 5 (left). Refractivity as a function of height in the nighttime atmosphere of Venus.

Fig. 6 (below). Pressure as a function of height in the atmosphere of Venus; (a) nightside profile from pseudoinversion results and (b) dayside profile from direct inversion.

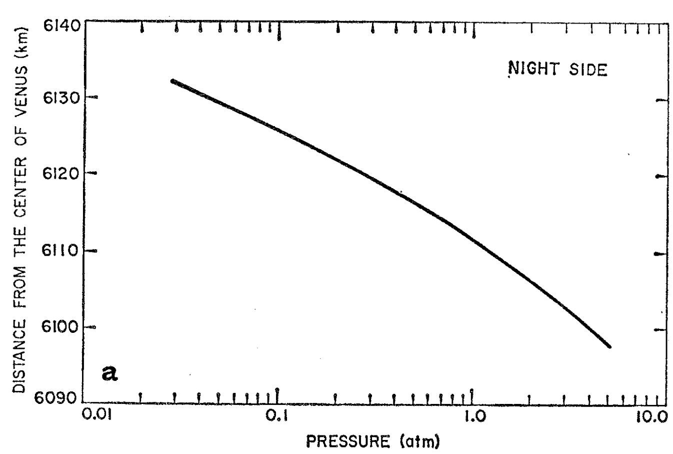

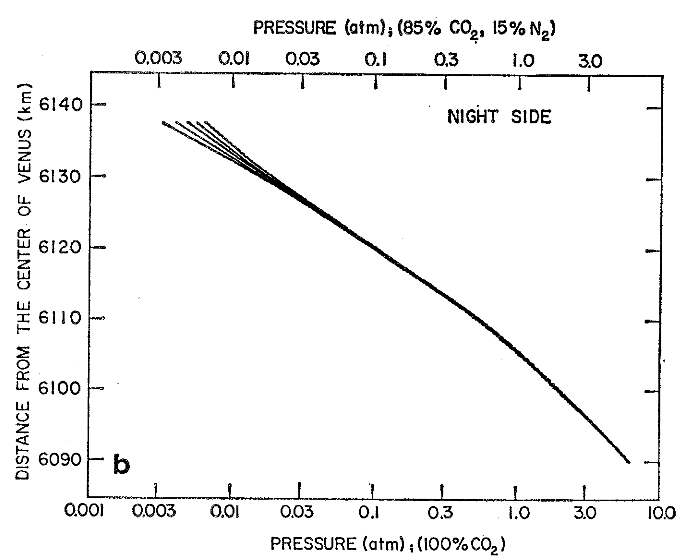

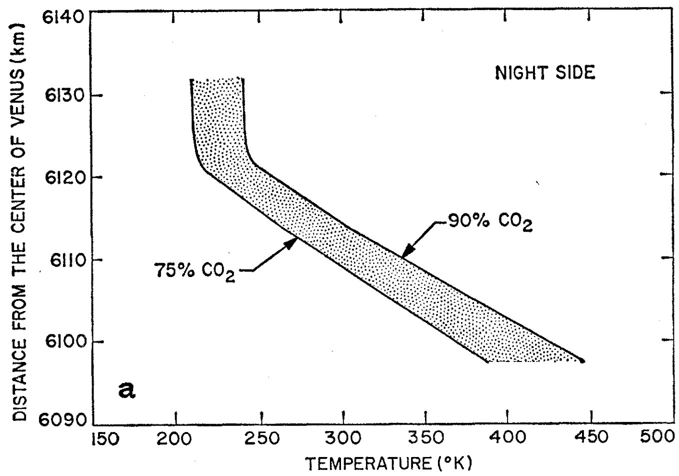

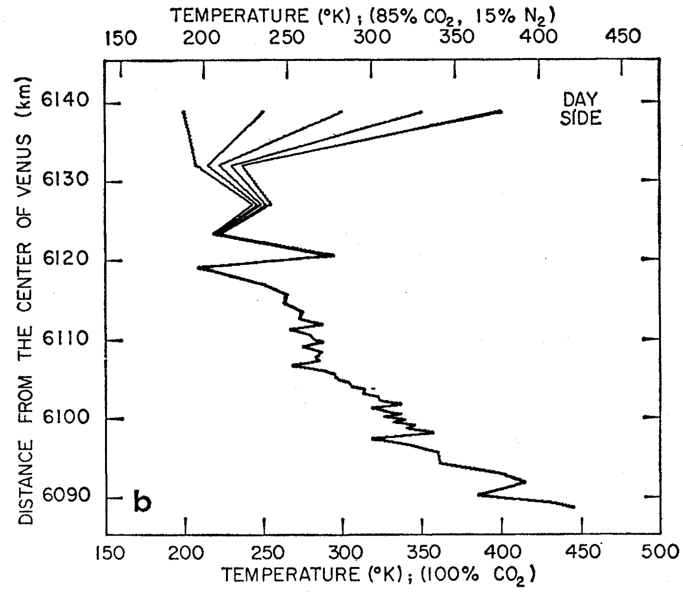

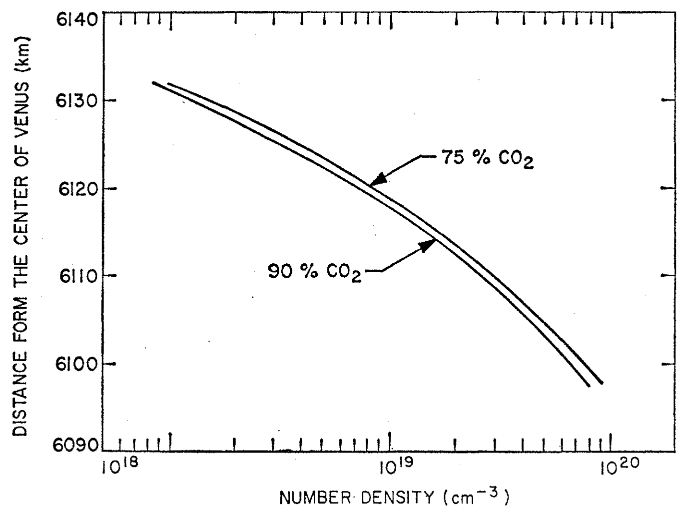

Fig. 7 (above). Temperature as a function of height in the nightside atmosphere of Venus (a) from pseudoinversion and (b) from direct inversion.

Fig. 8 (left). Number density as a function of height in the lower nightside atmosphere of Venus.

would be less than the effective temperature. If one assumes, then, that 230°K is the upper limit of temperature in the region in which the scale height of 5.4 ± 0.2 km is measured, the range of mean molecular weight is 39.0 to 42.0, corresponding to percentages of carbon dioxide of about 69 to 87 percent, provided that the balance of the atmosphere is composed of nitrogen. If heavier gases are present, the amount of CO_2 may be lower, and if light gases are present, the amount of CO_2 would have to be correspondingly higher. Thus, the measurement of scale height in the upper neutral atmosphere has provided an estimate of composition.

A profile of the refractivity in the nightside atmosphere as a function of height is shown in Fig. 5. This reduction is based only on the closed-loop data, and consequently the profile only extends to a radial distance of about 6095 km. Because of present uncertainties in the orbit of the probe, the values of radial distance for any given value of refractivity may change by about ±7 km; however, the nature of the profiles should remain essentially unaltered. When the open-loop data will be added, it will extend these profiles to the limit of measurement. However, this limit is likely to be only a few kilometers below the present minimum altitude, because of the rapid change of refractivity and its derivative in this region.

To compute pressure and temperature from refractivity, it is necessary to specify the composition. On the basis of the preceding discussion, it was decided to restrict the range of CO_2 abundance to 75 to 90 percent. Since the ratio of refractivity and molecular weight for CO_2 and N_2 are very similar, the computed pressure profiles for the two extreme compositions are coincident to the accuracy of illustration (Fig. 6). Figure 6a shows a nightside profile obtained from the results of the pseudoinversion program, and Fig. 6b is based on the direct inversion (*5*). The resulting profiles are quite similar, and the pressure at the present limiting minimum radial distance of 6095 km is about 5 atm.

The variation of temperature in the lower atmosphere is presented in Fig. 7. Part (a) again shows the temperature profiles in the nightside atmosphere computed from the results of the pseudoinversion program for CO_2 abundance of 75 and 90 percent, with the balance assumed to be nitrogen. Part (b) shows the dayside profile computed by the method of direct inversion (*5*). Again the results of the two very different reduction methods are essentially similar, showing a constant temperature above the tropopause at about 6120 km radial distance and a rapid increase of temperature with decreasing altitude below that level. In the case of 90 percent CO_2, the temperature is about 245°K above the tropopause, and the maximum is about 450°K at 6095 km. For 75 percent CO_2, the temperatures are correspondingly lower, starting at about 215°K above the tropopause and increasing to about 400°K at 6095 km. These temperatures are felt to be good upper and lower limits for the actual temperatures in the regions of the nightside atmosphere that were probed by the S-band occultation experiment. The number density was also computed for the two limiting abundances of CO_2, and the results are shown in Fig. 8.

Although the profiles of temperature and pressure do not extend to the surface of Venus, one is tempted to extend them to the region apparently measured by the Soviet Venera-4 probe. Thus, if these profiles are extended to the region of 15 to 22 atm of pressure and about 550°K in temperature as reported in *Izvestia*, the resulting radial distance is found to be about 6080 ± 10 km. If this is indeed the surface radius, it differs quite markedly from the surface radius of 6056 ± 1.5 km as established from analysis of planetary radar data (*6*).

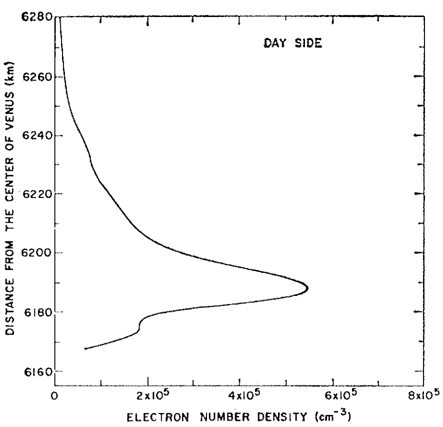

Fig. 9. Electron density in the daytime ionosphere.

The dayside ionization profile shows a distinct layer with a peak density between 5×10^5 to 6×10^5 electrons/cm^3 near 6190 km. There is also clear evidence of a minor layer approximately 15 km below the ionization maximum (Fig. 9).

Just above the ionization peak the plasma scale height is about 13 km, a value corresponding to a plasma temperature of about 300°K, if temperature gradients are negligible and if CO_2^+ is the principal ion. The plasma scale height on the ionospheric topside is increasing with increasing altitude, an indication of a higher plasma temperature or a change to a lighter ion at greater altitude, or both.

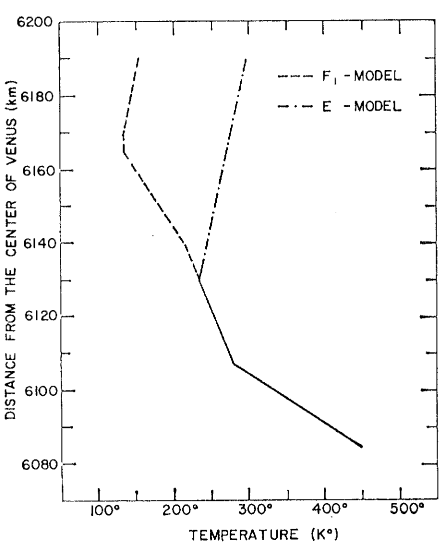

Fig. 10. Temperature in the atmosphere of Venus for F_1 and E ionosphere models.

By analogy with the formation of ionization layers in the terrestrial atmosphere one can interpret the dayside ionization peak with three types of models. As in the case of Mars (*7*) these three classes of models are designated as F_2, F_1, and E.

The F_2, or Bradbury models are based on the assumption that the observed ionization peak results from a rapid upward decrease of the ion-recombination loss coefficients together with downward diffusion of plasma. In the F_2 models, the electron-density peak is above the region where most of the electron production and recombination occurs.

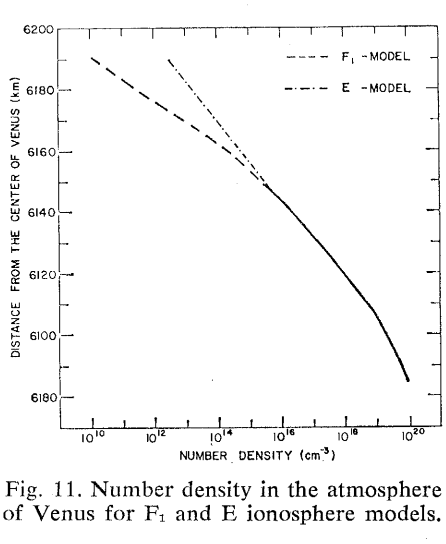

Fig. 11. Number density in the atmosphere of Venus for F_1 and E ionosphere models.

The F_1 and E models are based on the assumption that the observed ionization profile is a Chapman-type layer in which the peak coincides with the electron production peak caused by extreme solar ultraviolet and x-rays respectively.

The ultraviolet photometer observed no atomic oxygen on Venus (*8*). Thus, one can apparently rule out F_2 models that are based on atomic oxygen being the principal constituent at the ionization peak. Examples of F_1 and E models are illustrated in Figs. 10 and 11. The temperature and number-density profiles below 6130 km (solid line) were obtained from the refractivity measurements in the lower neutral atmosphere for the case of 100 percent CO_2. The dashed and dotted curves above 6130 kilometers represent extrapolations of the measurements in the lower atmosphere up to the level of the ionization peak. The minor layer may have been produced by x-rays and solar protons in the F_1 and E models, respectively.

These results are based on data available about 15 November 1967. They will be improved and refined in the future as more of the open-loop data become available and reduction methods are made more efficient. Among the results that will be available in the near future are complete profiles of refractivity, pressure, temperature, and number density derived from both closed-loop and open-loop data from both the entry (nighttime) and exit (daytime) data. Further study of these results will enable us to draw conclusions regarding the evolution of the lower atmosphere and the processes at work in the ionosphere.

ARVYDAS KLIORE
GERALD S. LEVY
DAN L. CAIN

Jet Propulsion Laboratory, California Institute of Technology, Pasadena, California

GUNNAR FJELDBO

Stanford Center for Radar Astronomy, Stanford University, Stanford, California

S. I. RASOOL

Institute for Space Studies, Goddard Space Flight Center, New York

References and Notes

1. A. Kliore, D. L. Cain, G. S. Levy, V. R. Eshleman, G. Fjeldbo, F. D. Drake, *Science* **149**, 3689 (1965).
2. A. Kliore, D. A. Tito, D. L. Cain, G. S. Levy, *J. Spacecraft Rockets* **4**, 10 (1967).
3. G. Levy, T. Otoshi, B. Seidel, *I.E.E.E. Inst. Electric. Electron. Eng. Trans. Instrumentation Measurement* **IM-6**, 2 (1967).
4. G. Fjeldbo and V. R. Eshleman, *J. Geophys. Res.* **70**, 13 (1965).
5. G. Fjeldbo and V. R. Eshleman, *Report No. SU-SEL-67-109*, Stanford University, November 1967.
6. M. E. Ash, I. I. Shapiro, W. B. Smith, *Astron. J.* **72**, 338 (1967).
7. G. Fjeldbo, W. C. Fjeldbo, V. R. Eshleman, *Science* **153**, 1518 (1966).
8. C. A. Barth, J. B. Pearce, K. K. Kelly, L. Wallace, W. G. Fastie, *Science*, this issue.
9. We thank the Mariner Project and Deep Space Net personnel of JPL for their excellent performance in the acquisition of data. We also thank D. Nixon, P. Parsons, and D. W. Kendall of JPL for reduction of data. This report presents the results of one phase of research carried out at the Jet Propulsion Laboratory, California Institute of Technology, under NASA contract NAS7-100. The Stanford contribution was supported by JPL contract JPL-951520.

11 December 1967